



## Research paper

# Parametric analysis of mast guys within the elastic and inelastic range

Monika Matuszkiewicz<sup>1</sup>, Renata Pigoń<sup>2</sup>

**Abstract:** The paper concerns the computations of mast guys taking into account both geometric and physical nonlinearities. Experimental studies have been conducted, the aim of which was to determine  $\sigma - \varepsilon$  (stress – deformation) relation for steel rope and to determine the value of modulus of elasticity after its pre-stretching. Results of the research were used to create appropriate computational cable models within the elastic and inelastic range in SOFiSTiK software, based on FEM. The computational cable models were then used to perform parametric analyses of single cables with horizontal and diagonal chords and computations of a lattice guyed mast. The computational single cables results obtained in the SOFiSTiK software were confronted with the results obtained by the analytical method, based on the cable equation. The FEM analyses performed for single cables have proven usefulness of presented analytical procedure for computation of structures with cable elements (e.g. guyed masts) taking into account both the geometric and physical nonlinearity of the cables. It has been shown that while using steel ropes without pre-stretching, permanent deformations in the cables may occur, which affect the shape of the cable and may significantly reduce values of forces in the cables. This phenomenon can be particularly dangerous in the case of guyed masts, as it may affect the reduction in rigidity of the mast structure.

**Keywords:** experimental studies of cables, geometric nonlinearity, global static analysis, mast guys, physical nonlinearity

<sup>1</sup>BEng., PhD., DSc., Koszalin University of Technology, Faculty of Civil Engineering, Environmental and Geodetic Sciences, Śniadeckich 2, 75-453 Koszalin, Poland, e-mail: [monika.matuszkiewicz@tu.koszalin.pl](mailto:monika.matuszkiewicz@tu.koszalin.pl), ORCID: 0000-0002-7479-4013

<sup>2</sup>BEng., MSc., Koszalin University of Technology, Faculty of Civil Engineering, Environmental and Geodetic Sciences, Śniadeckich 2, 75-453 Koszalin, Poland, e-mail: [renata.pigon@tu.koszalin.pl](mailto:renata.pigon@tu.koszalin.pl), ORCID: 0000-0002-3190-0197

## 1. Introduction

Guyed masts are vertical, slender high-rise structures, built of a lattice or tubular shaft and supporting on several levels diagonal wire ropes. Mast structures are most often used to suspend transmitting and receiving radio and television antennas as well as wireless communication antennas. They can also be used as measuring masts, e.g. for wind speed and wind direction. Due to their slender structure guyed masts belong to the structures that are susceptible to deformations. Moreover, geometric non-linearity of guys supporting the mast shaft causes the entire structure to behave nonlinearly, i.e. the displacements of the mast shaft are nonlinearly dependent on the external load. The correct response of the mast structure to external load in this case can be obtained only in an iterative way, where the aim is to fulfill the equilibrium equations of the deformed structure. Such type of analysis recommended in European standard [1] is called a nonlinear analysis of the second order theory.

Physical nonlinearity concerns structures where brand new ropes, without pre-stretching, were used to make cables. Such cables are characterized by a nonlinear stress – deformation relation, which results in a variable modulus of elasticity  $E$ , which in turn determines tensile stiffness of the rope. Including in computations of the constant modulus of elasticity would require pre-stretching of all used ropes, which is difficult to achieve especially in the case of guyed masts of considerable height.

At present, taking into account the geometric nonlinearity of cables in structure is not a computation problem for researchers. In the computations of e.g. guyed masts, the easiest effective way is to divide the curvilinear guy into appropriate number of straight elements and to perform spatial analysis of the structure in accordance with FEM methods. Such a procedure, used i.a. in the works [2, 3] results from availability of commercial computation software enabling performance of the geometrically nonlinear analysis for cable-bar structures. Another way is to consider in the computations the curvilinear shape of mast guys as the result of their inter-node load. The computation methods used in this case are usually based on iterative methods of modification of mast guy stiffness [4–7].

The vast majority of research works on guyed masts is based on computations within the linear-elastic range, limited to taking into account geometric nonlinearity of the structures. The analysis of cable structures within the physically nonlinear range has been presented, for example, in [8, 9]. However, there is a significant group of works on the study of physical nonlinearity of steel ropes. In [10] a comparative analysis of a steel spiral strand rope subjected to axial-torsional load using analytical methods and FEM has been presented. The effect of inter-wire contact in the wire rope subjected to axial tension and torsion loads using the semi-analytical method has been presented in [11]. In [12] the results of theoretical calculations of a steel wire rope according to the Feyrer's and Costello's theories have been compared with the results of experimental research. A numerical model for cables based on FEM including friction has been described in [13].

In this study the authors used for the analyses the mechanical properties of spiral strand ropes determined on the basis of experimental studies during the static stretching test. The

computational cable models tested within the linear-elastic and inelastic range in SOFiSTiK software will be used subsequently for the analyses of guyed mast structures.

## 2. Experimental study

Mechanical properties of steel ropes are significantly affected by rope structure, i.e. the number of wires and the method of twisting the wires in the rope. Brand new ropes, without pre-stretching, tend to show so-called stretching, i.e. increasing the length under load, resulting in permanent deformations. The typical  $\sigma - \varepsilon$  relation for a rope without pre-stretching determined on the basis of the static stretching test is, therefore, nonlinear, and the modulus of elasticity of such a rope, defined as  $E = \Delta\sigma / \Delta\varepsilon$ , is variable in this case and depends on the current stress value. The pre-stretching process, consisting in cyclic loading and unloading of a rope, causes permanent deformations and results in a significant increase of the value of the rope elasticity modulus  $E$ . After pre-stretching, the rope behaves elastically, in the range of applied axial force, thus the value of modulus  $E$  is constant.

In order to show differences in the results of computations of guyed masts in which the spiral strand ropes without pre-stretching (inelastic range) and the pre-stretched ropes (elastic range) were adopted as guys, the experimental studies of a steel spiral rope had been carried out. A full description of the research and its results was presented at the conference of young scientists in 2018 [14]. Below are briefly described the scope of the research and its results, which have been further used to perform analyses.

The subject of the experimental research was PG 40 spiral strand rope with the structure  $1 \times 37$ , diameter 20.1 mm and cross-section  $A = 237 \text{ mm}^2$ , manufactured by PFEIFER Seil – Und Hebetchnik GmbH [15]. The minimum rope breaking force specified by the producer is 367 kN. The tensile strength of rope wires is  $f_{u,k} = 1770 \text{ MPa}$ ; the wires have been protected with GALFAN anticorrosion zinc coating.

15 rope samples featuring length of 1.24 m, based on the standard [16] were prepared for tests. Ends of the ropes were anchored in conical bushes (Figs. 1, 2), made of S355 steel grade, in accordance with the standard [17]. The cold socketing compound named WIRELOCK, manufactured by the Millfield Group [18], was used as a socketing media. The experimental tests were carried out in the Laboratory of Material Strength and Building Structures of Koszalin University of Technology. Inspekt 600 testing machine by Hegewald Und Peschke MPT GmbH was used. The device is computer controlled using closely

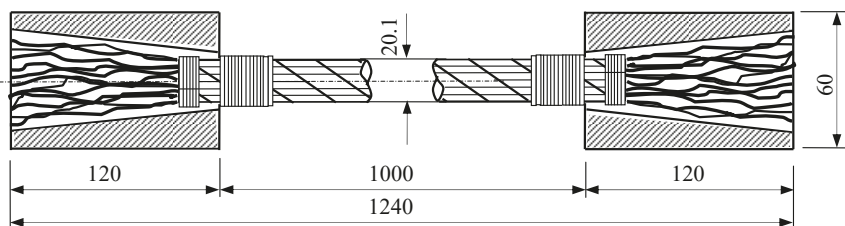


Fig. 1. Dimensions of a rope sample with conical bush [mm]

cooperating software called H&P Labmaster, which is responsible, among other things, for saving, managing and processing of the measurement data.



Fig. 2. Rope samples prepared for tests

View of the rope sample in the testing machine is presented in Fig. 3.

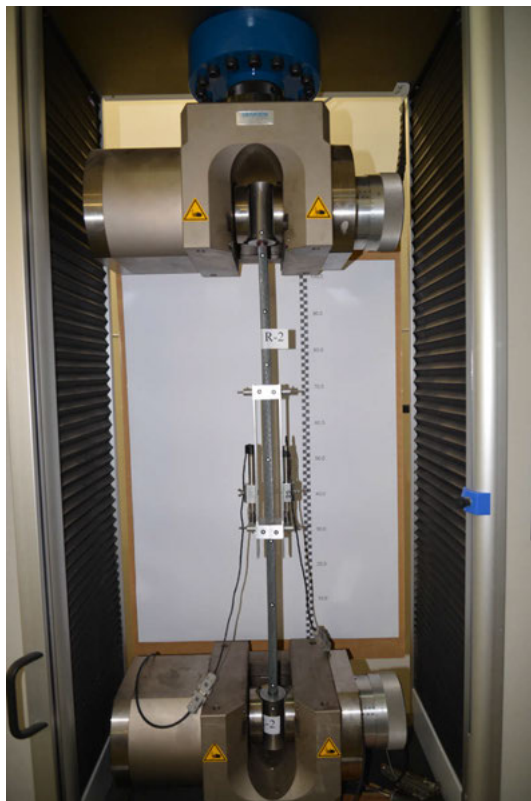


Fig. 3. View of the rope sample in testing machine

The tests included:

- determination of  $\sigma - \varepsilon$  relation for the rope during the static stretching test based on the measured values of force – rope elongation,
- finding the constant (standard) value of the rope elasticity coefficient  $E$  after its pre-stretching,
- determination of the real value of the rope breaking force.

The tests were conducted in compliance with the guidelines set out in the standard [19]. In order to eliminate the initial non-straightness, the rope samples mounted in the testing machine were initially subjected to force  $P_0 = 5 \div 10$  kN. The pre-stretching process was carried out on six rope samples in accordance with the recommendations set out in the standard [1] regarding guys pre-stretching. This process consisted in cyclic loading and unloading of the rope (minimum 10 cycles) within the range from 10% to 50% of the nominal breaking force. The tested rope samples were loaded 12 times in the testing machine up to the force value equal to 183.5 kN and then unloaded. As a result of this process, permanent deformations appeared in the rope samples, visible on the section A – C of the  $\sigma - \varepsilon$  curve (Fig. 4), while the section B – C during unloading and re-loading is practically linear. Hence, the constant (standard) value of the rope elasticity modulus was determined. For six tested samples the arithmetic mean value of the rope elasticity modulus was equal to 158 GPa, therefore, a good correlation with the standard recommendations [20] regarding the assumption of constant elasticity modulus of spiral strand ropes  $E = 150 \pm 10$  GPa was obtained.

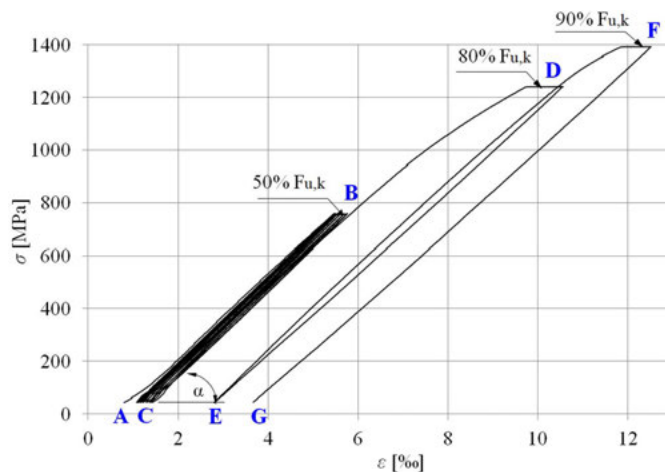


Fig. 4. Graph of nonlinear relation stress – deformation of the rope during cyclic loading and unloading

Six consecutive rope samples were used to determine the nonlinear  $\sigma - \varepsilon$  relation during the static tensile test. The loading was commenced with initial force of 5 kN and increased at a rate of 1 kN/s until the breaking force value specified by the producer equal to 367 kN. The graph of  $\sigma - \varepsilon$  relation for the rope is shown in Fig. 5.

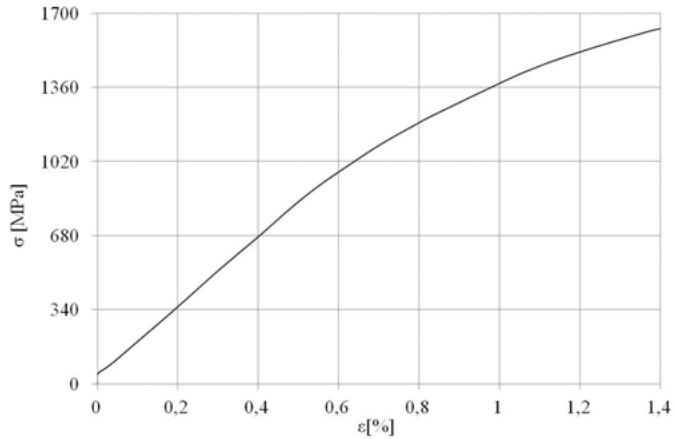


Fig. 5. Relation  $\sigma - \epsilon$  for the tested rope subjected to static tensile test

All of the 15 rope samples were loaded until rupture of individual wires in the rope had occurred. The samples were destroyed in the middle of the span, which proves that the anchoring was correctly made (Fig. 6). The highest value of the obtained breaking force was equal to 430.8 kN, and the lowest – 414.6 kN. The average value of the breaking force was obtained equal to 425.3 kN.



Fig. 6. View of broken rope samples

The constant (standard) value of the elasticity modulus  $E = 158$  GPa, determined in the tests, was used in further analyses to compute the cables within the elastic range, while  $\sigma - \epsilon$  nonlinear relation for the rope without pre-stretching was approximated by the 4<sup>th</sup> degree polynomial described by the following equation (2.1):

$$(2.1) \quad \sigma(\epsilon) = 25.963 + 1590.237\epsilon + 500.756\epsilon^2 - 1107.53\epsilon^3 + 376.147\epsilon^4 \quad [\text{MPa}]$$

The equation was used, in turn, to develop a physically nonlinear cable model where modulus  $E$  is determined in a particular iteration based on the current values of stresses and deformations. Comparison of the experimental results and the  $\sigma - \varepsilon$  curve described by the adopted polynomial is shown in Fig. 7.

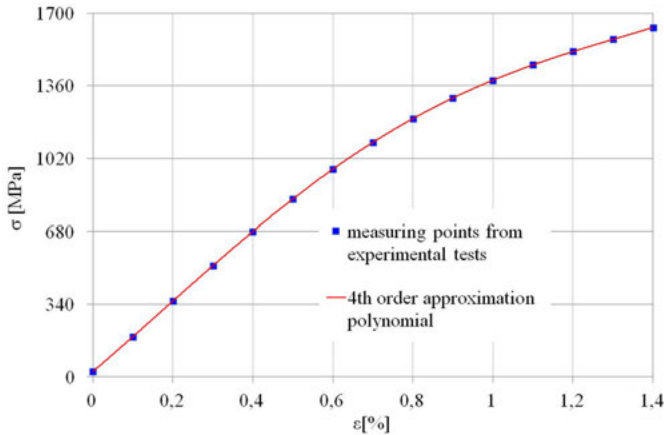


Fig. 7. Comparison of the experimental results and the adopted polynomial approximating  $\sigma - \varepsilon$  relation for the tested rope

### 3. Cable equation

The relationship between cable length  $s_0$  before installation and its length  $s$  under load is shown in the following equation (3.1) [4, 21]:

$$(3.1) \quad s = s_0 + \Delta s + \Delta s_t$$

where  $\Delta s$  is the elastic elongation of the cable and  $\Delta s_t$  – the elongation (or shortening) of the cable due to temperature change.

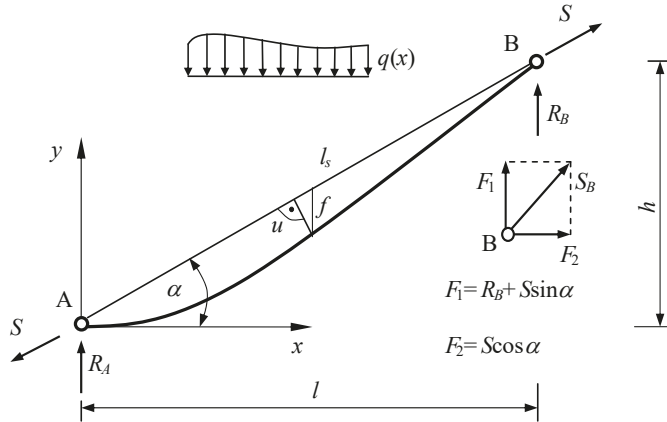
Assuming that the shape of the cable under load is described by the catenary equation (3.2) [4, 22, 23]:

$$(3.2) \quad y = k \left[ \cosh \left( \frac{x}{k} \right) - 1 \right]$$

( $k = S/g$  [m],  $S$  – cable force (Fig. 8),  $g$  – cable self-weight), the so called exact cable equation (3.3) from equation (3.1) after transformations is obtained, on the basis of which cable force  $S$  can be determined [9]:

$$(3.3) \quad \frac{2S}{g} \sinh \frac{l \cdot g}{2H} = s_0 (1 + \alpha_t \Delta T) + \frac{S^2}{2E \cdot A \cdot g} \left[ \frac{l \cdot g}{S} + \sinh \frac{l \cdot g}{S} \right]$$

However, in practical computations, with some simplifying assumptions, it is more convenient to assume that the cable overhang line is determined by the second degree

Fig. 8. Slant cable (guy) under  $q(x)$  load

parabola (the so-called technical theory of the cable applies). On this assumption an approximate equation (3.4) of mast guy (slant cable) was derived in [4], based on the current length of the cable chord:

$$(3.4) \quad S^3 + S^2 EA \left[ 1 - \frac{1}{s_0} (l_s - \alpha_t \Delta T s_0) \right] = \frac{EA \cos \alpha}{2s_0} \int_0^l [Q(x)]^2 dx$$

where:  $S$  – force acting in the cable chord direction (Fig. 8),  $s_0$  – length of unloaded cable,  $E$  – cable modulus of elasticity,  $A$  – rope metallic cross section,  $\alpha_t$  – linear extension factor ( $\alpha_t = 0.000012$  1/K),  $\Delta T$  – change of temperature,  $l_s$  – length of cable chord,  $Q(x)$  – shear force equation as for a simply supported beam with span  $l$  subjected to load  $q(x)$ .

In situation where length of the cable  $s_0$  corresponds to a certain initial value of force  $S_0$ , equation (3.4) can be expressed in the following form (3.5):

$$(3.5) \quad S^3 + S^2 \left[ EA - S_0 - \frac{EA}{s_0} (l_s - \alpha_t \Delta T s_0) \right] = \frac{EA \cos \alpha}{2s_0} \int_0^l [Q(x)]^2 dx$$

In the case of guy unloading, the initial state of the guy is the computed value of force  $S_k$  of the total load and the corresponding final length of the guy  $s_k$ . Therefore, equation (3.5) takes the following form (3.6):

$$(3.6) \quad S^3 + S^2 \left[ EA - S_k - \frac{EA}{s_k} (l_s - \alpha_t \Delta T s_k) \right] = \frac{EA \cos \alpha}{2s_k} \int_0^l [Q(x)]^2 dx$$

The final guy length can be determined from [4]:

$$(3.7) \quad s_k = l_s + \frac{\cos \alpha}{2S_k^2} \int_0^l [Q(x)]^2 dx$$



The equations presented above show a good convergence with the exact solution in the case of cables with small overhangs (when the ratio of the guy sag  $f$  to span  $l$  is less than 0.1) and low angles of the cable chord inclination to the horizontal ( $\alpha < 60^\circ$ ), which conditions for most structures of guyed masts are met [4]. In computations in the elastic range the value of  $E$  modulus of elasticity is constant. In the computations in the inelastic range, it is assumed that the curvilinear relation  $\sigma - \varepsilon$  applies during loading of the guy, so the modulus  $E$  depends on the values of stresses and strains of the guy, and during unloading and re-loading, the constant value of the modulus  $E$  is constant. Proper value of the modulus of elasticity  $E$  can be determined based on  $\sigma - \varepsilon$  relation using the iterative secant method (successive approximations method) [9].

## 4. Guys modelling and computation method using sofistik software

SOFiSTiK commercial software allows, for example, to perform a fully nonlinear analysis of bar structures based on FEM [24]. It consists of several modules interconnected through a common database (CDBase). Depending on the considered type of structure, modules which are used, are responsible for:

- adoption of initial assumptions (PREPROCESSING),
- carrying out calculations (PROCESSING),
- presentation and further processing of the obtained results (POSTPROCESSING).

Description of the structure is best done with use of TEDDY text editor, in which all the parameters of the structure are defined by text code (CANDIP) in an alphanumeric format. In AQUA module, which is intended to define the material properties and cross-sections, the range in which cable element works, should be specified. In the case of the analysis within the linear-elastic range, a constant value of elastic modulus  $E$  for cables (adopted on the basis of experimental tests of rope  $E = 158$  GPa) is assumed.

When analysis within inelastic range is chosen, using SSLA (Stress – strain curves) command, the curvilinear characteristic  $\sigma - \varepsilon$  of the rope is introduced by defining the coordinates of up to 20 points (stress – SIG in [N/mm<sup>2</sup>], strain – EPS in [1/1000]).

In SOFiMSHA module, the geometry of the structure is described.

First of all a global coordinate system (e.g. a spatial system) should be defined, then groups of elements are introduced, next nodes and boundary conditions are defined.

In the case of cable elements – the division into  $n$ -components is given (in the presented examples of computations, the division into 30 elements was used).

The load of structure elements is defined in SOFILOAD module. The self-weight of the guys, initial guys forces, other loads and, if necessary, the unloads, should be given separately. Computations are carried out in ASE module on the basis of declared load tests. In the case of structures with cables – in the first ASE module, the self-weight of the structure and initial forces of the cables should be taken into account. It is the main module, the base for further combinations. The appropriate type of analysis should be chosen.

In the case of structures with cable elements, it is best to assume TH3 – the equivalent of the classical second-order theory. The solution of the geometrically nonlinear problem is possible in the software in an iterative way. A modified Newton's method (iteration-incremental method) is used, in which the stiffness matrix is updated at each iteration step and the speed of finding a solution is increased thanks to the Crisfield method. The module should include, among other things, the number of iterations, the increase of given load and the accuracy of solution. In order to activate calculations of cables within the inelastic range, NSTR (Non-linear stress and strain) command should be entered.

## 5. Computation examples

The above-presented models and computation procedures for structures with cable elements in SOFiSTiK software within the linear elastic and inelastic range were tested on examples.

### Example 1.

Compute a horizontal cable force  $S$  under given load  $g + p$  (Fig. 9). Cross section  $A = 2.37 \text{ cm}^2$ , horizontal distance between supports  $l = 60 \text{ m}$ , unloaded cable length  $s_0 = 60 \text{ m}$ , permanent load  $g = 1.0 \text{ kN/m}$ , variable load  $p = 1.0 \div 5.0 \text{ kN/m}$ .

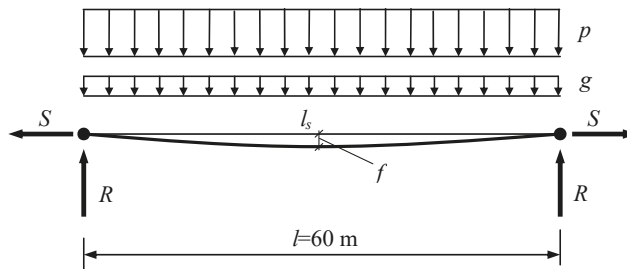
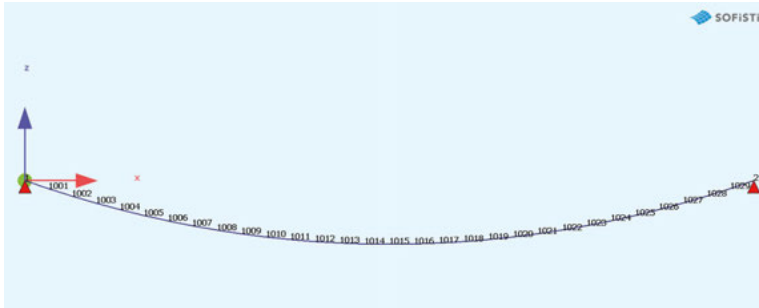
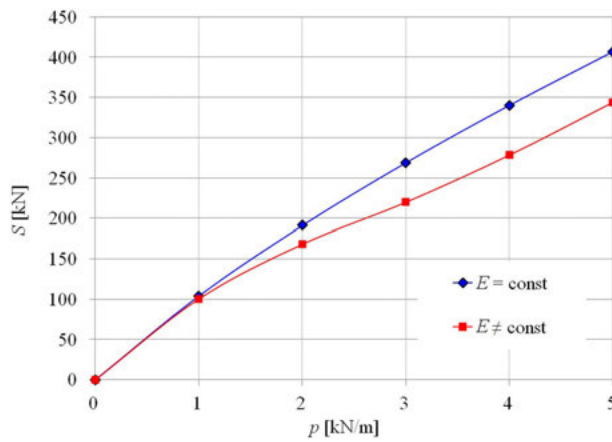


Fig. 9. Cable under load  $g$  and  $p$

The problem was solved in two variants. In the first one, it was assumed that the modulus of cable elasticity  $E$  is constant and amounts to 158 GPa. In the second variant, it was assumed that during load application, relation  $\sigma - \varepsilon$  for the rope is described by equation (1), and during rope unloading, constant modulus of elasticity  $E = 158 \text{ GPa}$  applies.

Model of a horizontal cable prepared in SOFiSTiK software under  $g + p$  load is presented in Fig. 10.

Figure 11 shows graphical dependence between given load and cable force value  $S$  computed in the SOFiSTiK software in both variants. Table 1 presents calculated cable guy sags  $f$ . Additionally, for comparative purposes, computed cable force  $S$  in SOFiSTiK software was confronted with the results obtained based on cable equations (3.4) and (3.6) and summarized in Table 2.

Fig. 10. Model of a horizontal cable in SOFiSTiK software under  $g + p$  loadFig. 11. Effect of load change  $q = g + p$  on cable force  $S$  change [kN]Table 1. Cable guy sag  $f$  [m] comparison within the linear-elastic and inelastic range

Range		$p = 0$ kN/m	$p = 1$ kN/m	$p = 2$ kN/m	$p = 3$ kN/m	$p = 4$ kN/m
Linear-elastic	Load ( $g + p$ )	2.54	3.21	3.68	4.05	4.37
	Unload $g$	–	2.54	2.54	2.54	2.54
Inelastic	Load ( $g + p$ )	2.54	3.25	3.92	4.55	4.97
	Unload $g$	–	2.54	2.83	3.25	3.45

Comparing the results of cable forces computation  $S$  in SOFiSTiK software and based on cable equation, a good convergence within the linear-elastic range can be noticed – the differences do not exceed 1%. Slightly larger differences (about 2%) were obtained for

Table 2. Computed cable force  $S$  [kN]: a) using SOFiSTiK software, b) based on the cable equation: load – equation (3.4), unload – equation (3.6)

Range			$p = 0$ kN/m	$p = 1$ kN/m	$p = 2$ kN/m	$p = 3$ kN/m
Linear-elastic $E = \text{const}$	Load $(g + p)$	a)	176.9	281.1	368.2	445.9
		b)	177.7	282.2	369.7	447.9
	Unload $Ug$	a)	–	177.8	177.8	177.8
		b)	–	178.0	178.0	178.0
Inelastic $E \neq \text{const}$	Load $(g + p)$	a)	176.9	277.4	345.3	396.9
		b)	177.7	280.2	354.2	405.5
	Unload $g$	a)	–	178.2	160.1	139.5
		b)	–	176.1	163.5	141.9

$E \neq \text{const}$ . This can be explained by application of different cable computational models and different iterative methods applied for solving the problem of geometrical and physical cable nonlinearity in SOFiSTiK software and in calculations based on the approximate cable equation. In both cases, however, a significant difference in behavior of the cable with linear elastic and inelastic characteristics can be noticed. In a cable with inelastic characteristic along with the increase in load, permanent deflections increase too, which causes reduction of the force in the cable. After unloading, such cable does not return to the original configuration, so cable guy sag is bigger than in the case of assumption  $E = \text{const}$ .

**Example 2.**

Compute a slant cable force  $S$  under given load  $g + p$  (Fig. 12). Cross section  $A = 2.37 \text{ cm}^2$ , horizontal distance between supports  $l = 60 \text{ m}$ , unloaded cable length  $s_0 = l_s$ , permanent load  $g = 1.0 \text{ kN/m}$ , variable load  $p = 1.0 \div 5.0 \text{ kN/m}$ . The angle of cable

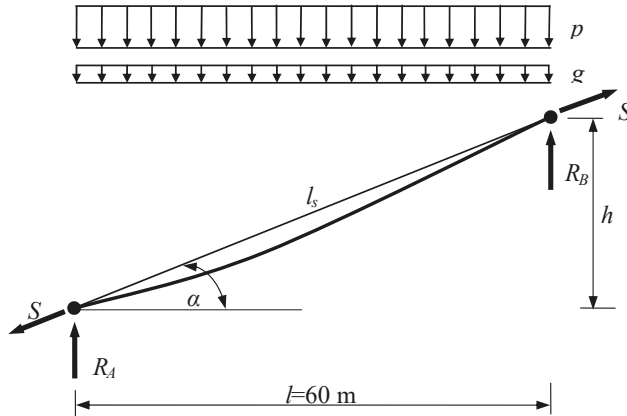


Fig. 12. A slant cable under  $g$  and  $p$  load

chord inclination to horizontal  $\alpha$  is  $45^\circ$ ,  $50^\circ$ ,  $55^\circ$  and  $60^\circ$ . As in the previous example, the computations were carried out in two variants – for  $E = \text{const}$  and for  $E \neq \text{const}$ .

The computed values of cable force  $S$  are presented in Table 3. Additionally, for  $\alpha = 45^\circ$ , computation results obtained from analytical method based on cable equation are given in brackets.

Table 3. Computed cable force  $S$  [kN]

$\alpha = 45^\circ$						
Range		$p = 1$ kN/m	$p = 2$ kN/m	$p = 3$ kN/m	$p = 4$ kN/m	$p = 5$ kN/m
Linear-elastic $E = \text{const}$	Load ( $g + p$ )	223.3 (223.9)	293.3 (293.5)	356.2 (355.5)	414.3 (412.5)	464.8 (465.8)
	Unload $g$	140.7 (141.2)	140.7 (141.2)	140.7 (141.2)	140.7 (141.2)	140.7 (141.2)
Inelastic $E \neq \text{const}$	Load ( $g + p$ )	222.7 (226.3)	285.5 (290.2)	332.9 (342.9)	370.6 (385.2)	414.9 (411.8)
	Unload $g$	153.5 (143.6)	136.2 (138.3)	122.5 (129.7)	110.4 (117.8)	104.3 (100.2)
$\alpha = 50^\circ$						
Range		$p = 1$ kN/m	$p = 2$ kN/m	$p = 3$ kN/m	$p = 4$ kN/m	$p = 5$ kN/m
Linear-elastic $E = \text{const}$	Load ( $g + p$ )	210.3	276.6	333.4	388.1	439.6
	Unload $g$	131.5	131.5	131.5	131.5	131.5
Inelastic $E \neq \text{const}$	Load ( $g + p$ )	211.6	273.6	318.0	364.5	400.1
	Unload $g$	144.1	128.8	118.4	108.1	100.4
$\alpha = 55^\circ$						
Range		$p = 1$ kN/m	$p = 2$ kN/m	$p = 3$ kN/m	$p = 4$ kN/m	$p = 5$ kN/m
Linear-elastic $E = \text{const}$	Load ( $g + p$ )	196.0	258.5	315.1	367.8	407.7
	Unload $g$	123.1	123.1	123.1	123.1	123.1
Inelastic $E \neq \text{const}$	Load ( $g + p$ )	195.8	254.9	304.1	337.5	378.2
	Unload $g$	135.1	121.7	112.8	101.8	95.6
$\alpha = 60^\circ$						
Range		$p = 1$ kN/m	$p = 2$ kN/m	$p = 3$ kN/m	$p = 4$ kN/m	$p = 5$ kN/m
Linear-elastic $E = \text{const}$	Load ( $g + p$ )	180.5	238.7	284.9	332.9	378.4
	Unload $g$	112.9	112.9	112.9	112.9	112.9
Inelastic $E \neq \text{const}$	Load ( $g + p$ )	180.3	236.5	278.5	316.5	354.9
	Unload $g$	124.6	113.5	105.4	95.7	89.2

Therefore, it can be noted that also in the case of slant cable computation (e.g. mast guy) convergence of computation results from SOFiSTiK software and calculations based on the approximate cable equation are satisfactory (< 1% difference for  $E = \text{const}$  and about 2% difference for  $E \neq \text{const}$ ).

**Example 3.**

The subject of the analysis is a 140 m high mast with two guy levels at heights of 60 m and 120 m respectively (Fig. 13). The mast shaft was designed as S355 steel in form of three-walled space truss with the axial spacing of legs equal to 1.8 m. Circular hollow sections  $\varnothing 168.3/14.2$  mm were used as leg members, and as mast face lacing – circular hollow sections  $\varnothing 76.1/4$  mm. The mast guys were designed of spiral strand steel ropes PG 551  $\times$  37 structure, diameter  $\varnothing 24.4$  mm and minimum breaking force  $N_{\text{min}} = 537$  kN. The assumed values of the initial guy forces at all levels amount to 40 kN. The mast location was assumed in the second category area as per [25]. It has been assumed that value of the base wind pressure is  $q_b = 2.81$  kN/m<sup>2</sup>. The mast structure has been qualified to the second reliability class, in accordance with [1], for which the partial factors for permanent loads are equal to 1.1 and for variable loads 1.4.

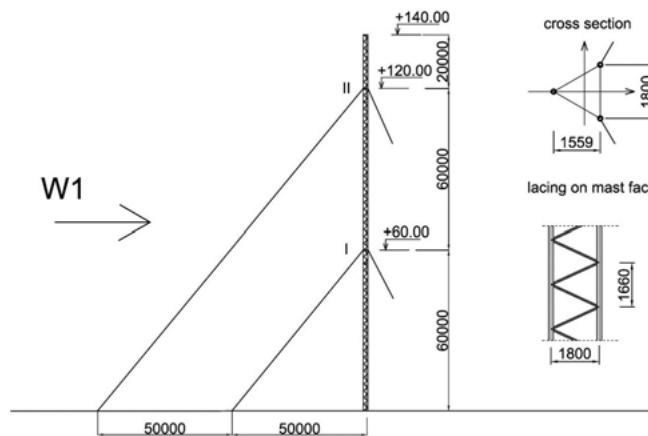


Fig. 13. Mast structure diagram

Own weight of structure and wind action for direction W1 were taken into account in the analysis (Fig. 13).

Static computations of the mast structure were performed using SOFiSTiK software in two variants – in the first one, it was assumed that the mast guys were initially pre-stretched, so constant value of the elasticity modulus  $E = \text{const} = 158$  GPa was assumed; in the second variant, it was assumed that the guys were made of brand new ropes, without pre-stretching, for which, during the load,  $\sigma - \varepsilon$  characteristic for the rope was described by equation (2.1) ( $E \neq \text{const}$ ), and during the unloading of the rope, the constant modulus of elasticity  $E = 158$  GPa applied.

The mast shaft was modeled in SOFiSTiK software using a 3D beam-column model, with equivalent geometrical and strength characteristics (Fig. 14). The guys were modeled as cable elements with division into 30 parts along the guy length.

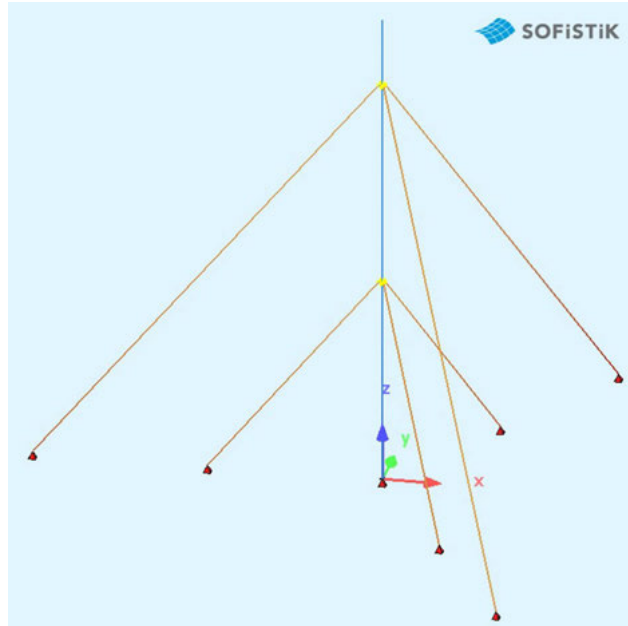


Fig. 14. Mast diagram in SOFiSTiK software

The most visible differences in computations result for the structure for as per variant I ( $E = \text{const}$ ) and variant II ( $E \neq \text{const}$ ) pertain to maximum force values of the mast guys on the windward side (direction of wind action on the guy  $0^\circ$ ) (Table 4) and the geometry of the deformed structure (Figs. 15, 16).

Table 4. Maximum mast guy forces [kN]

Guylevel	Direction of wind action on guy	Linear-elastic range $E = \text{const}$		Inelastic range $E \neq \text{const}$	
		Load ( $g + p$ )	Unload $g$	Load ( $g + p$ )	Unload $g$
I	$0^\circ$	489.4	37.9	496.6	24.5
	$120^\circ$	33.6	37.9	30.9	20.0
	$240^\circ$	33.6	37.9	30.9	20.0
II	$0^\circ$	535.2	40.0	525.5	23.0
	$120^\circ$	74.5	40.0	68.9	23.0
	$240^\circ$	74.5	40.0	68.9	23.0

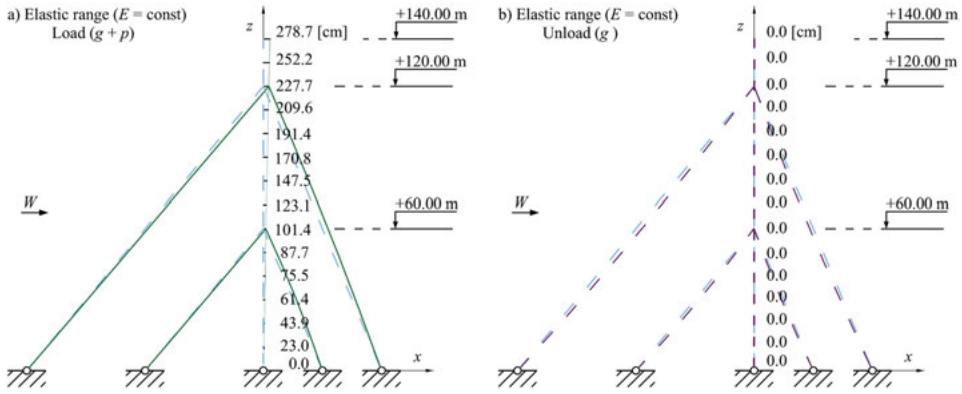


Fig. 15. Maximum horizontal displacements of mast shaft nodes – computations within the elastic range

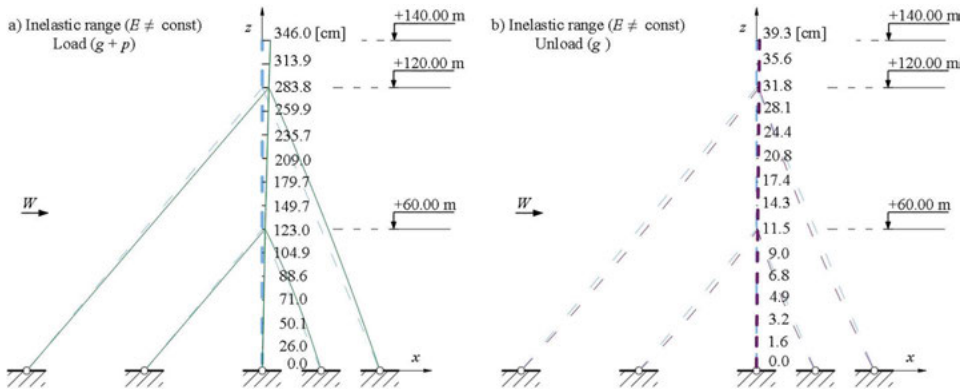


Fig. 16. Maximum horizontal displacements of mast shaft nodes – computations within the inelastic range

In variant I, the maximum values of guy forces of the windward side are higher, and after unloading the mast structure returns to its initial state, while in variant II values of the guy forces are smaller, horizontal deflection of the mast shaft is much greater, and after unloading, due to permanent deformations in the guys, the mast shaft remains tilted.

The maximum value of the mast guy force in the second variant of computations was 525.5 kN, which corresponds to the stresses equal to 151.47 kN/cm<sup>2</sup>. Taking into account the strains of the rope at the level of 1.23%, it is possible to check (e.g. Fig. 5) at which point of the curve  $\sigma - \varepsilon$  the guy is. In the first variant of computations ( $E = \text{const}$ ), the maximum value of the mast guy force was 535.2 kN, so the stresses level in the rope is greater and amounts to 154.24 kN/cm<sup>2</sup>.

In the analyzed example, inclusion in the computations of the physical non-linearity of the guys slightly decreased the values of normal forces in the mast shaft legs. The maximum



compressive force of 858.4 kN was recorded in the 2nd variant of computations, while in the 1st variant it was 906.1 kN (5% difference).

## 6. Final conclusions

The objectives of this paper were to check the possibility of using analytical procedure and SOFiSTiK commercial software for analysis of guyed masts, taking into account both the geometric and physical non-linearity of the guys. For this purpose, an appropriate computational model of the cable was defined, mechanical properties of which were determined based on experimental tests of a specific wire rope. The defined computation models of the cable within the linear-elastic and inelastic range were tested on simple examples, and computation results obtained from SOFiSTiK software were confronted with the results of the analytical method, based on the cable equation (technical theory of the cable). The obtained results turned out to be satisfactory – the differences in the computed values of cable force  $S$  in both examples for  $E = \text{const}$  did not exceed 1%. For  $E \neq \text{const}$  the differences were slightly bigger (about 2%), which can be justified by different iterative methods of the approximate solution.

Regardless of the cable chord angle of inclination to horizontal, the results of the cables computation within the linearly elastic and inelastic ranges differ significantly. In the first case, the cables are characterized by smaller deformations and greater cable forces, and in the second – by greater deformations and smaller cable forces. In addition, permanent deformations appear in the cables (the greater the load, the greater the values of these deformations), which do not disappear after unloading. In the case of guyed mast structures, this phenomenon may be so dangerous that it can cause significant reduction of the structure stiffness and loss of its verticality and so adversely affect functional properties of the mast. As design practice shows, the pre-stretching of new ropes of large lengths and diameters is often difficult to carry out. It is, therefore, justified to carry out analyses of masts structures taking into account also physical nonlinearity of the guys in the case when the guys were made of ropes without pre-stretching.

Results of the computations presented in the paper refer to a specific type of steel rope that has been tested in laboratory conditions and these are not supposed to be generalized. Considering steel rope of a different structure, the non-linear effects may be different – the more wires in the rope, the more non-linear characteristic of stress – strain. However, the method of proceeding presented in the paper, in the case of using ropes without pre-stretching, is universal.

## References

- [1] Eurocode 3. EN 1993-3-1: Design of steel structures. Part 3–1: Towers, masts and chimneys – Towers and masts. CEN Brussels 2006.
- [2] S.A. Sadrnejad, “Numerical solution of base shear in high tensioned cable antenna”, *Numerical Methods in Civil Engineering*, 2016, vol. 1, no. 2, pp. 21–30, <http://nmce.kntu.ac.ir/article-1-24-en.html>.

- [3] M. Matuszkiewicz, R. Orzłowska, “The influence of the second order effects on the results of computations of guyed masts with lattice shaft” (in Polish), *Inżynieria i Budownictwo*, 2017, no. 6, pp. 329–332.
- [4] Sz. Pałkowski, *Cable structures*. Warszawa: WNT, 1994.
- [5] Y.B. Yang, J.Y. Tsay, “Geometric nonlinear analysis of cable structures with a two-node cable element by generalized displacement control method”, *International Journal of Structural Stability and Dynamics*, 2007, vol. 7, no. 4, pp. 571–588, DOI: [10.1142/S0219455407002435](https://doi.org/10.1142/S0219455407002435).
- [6] H. Shi, H. Salim, “Geometric nonlinear static and dynamic analysis of guyed towers using fully nonlinear element formulations”, *Engineering Structures*, 2015, vol. 99, pp. 492–501, DOI: [10.1016/j.engstruct.2015.05.023](https://doi.org/10.1016/j.engstruct.2015.05.023).
- [7] P.M. Páez, B. Sensale, “Analysis of guyed masts by the stability functions based on the Timoshenko beam-column”, *Engineering Structures*, 2017, vol. 152, pp. 597–606, DOI: [10.1016/j.engstruct.2017.09.036](https://doi.org/10.1016/j.engstruct.2017.09.036).
- [8] Sz. Pałkowski, “Zur statischen Berechnung von Seilkonstruktionen im elastisch-plastischen Bereich”, *Bauingenieur*, 1992, no. 67, pp. 359–364.
- [9] M. Matuszkiewicz, “Computations of cable structures in the elastic-plastic range” (in Polish), *Inżynieria i Budownictwo*, 2003, no. 7, pp. 393–396.
- [10] F. Foti, A. de Luca di Roseto, “Analytical and finite element modeling of the elastic-plastic behaviour of metallic strands under axial-torsional loads”, *International Journal of Mechanical Sciences*, 2016, vol. 115–116, pp. 202–214, DOI: [10.1016/j.ijmecsci.2016.06.016](https://doi.org/10.1016/j.ijmecsci.2016.06.016).
- [11] F. Meng, Y. Chen, M. Du, X. Gong, “Study on effect of inter-wire contact on mechanical performance of wire rope strand based on semi-analytical method”, *International Journal of Mechanical Sciences*, 2016, vol. 115–116, pp. 416–427, DOI: [10.1016/j.ijmecsci.2016.07.012](https://doi.org/10.1016/j.ijmecsci.2016.07.012).
- [12] Y.A. Onur, “Experimental and theoretical investigation of prestressing steel strand subjected to tensile load”, *International Journal of Mechanical Sciences*, 2016, vol. 118, pp. 91–100, DOI: [10.1016/j.ijmecsci.2016.09.006](https://doi.org/10.1016/j.ijmecsci.2016.09.006).
- [13] B. Liang, Z. Zhao, X. Wu, H. Liu, “The establishment of a numerical model for structural cables including friction”, *Journal of Constructional Steel Research*, 2017, vol. 139, pp. 424–436, DOI: [10.1016/j.jcsr.2017.09.031](https://doi.org/10.1016/j.jcsr.2017.09.031).
- [14] R. Pigoń, “Experimental study of mechanical properties of steel cables”, in *The 2<sup>nd</sup> Baltic Conference for Students and Young Researchers (BalCon 2018), 20-23 April 2018, Gdynia, Poland*. MATEC Web of Conferences, 2018, vol. 219, no. 02004, DOI: [10.1051/mateconf/201821902004](https://doi.org/10.1051/mateconf/201821902004).
- [15] GmbH, Pfeifer Seil – und Hebetchnik. Pfeifer Tension Members. 2015, no. 10. [https://www.pfeifer.info/out/assets/PFEIFER\\_TENSION-MEMBERS\\_BROCHURE\\_EN.PDF](https://www.pfeifer.info/out/assets/PFEIFER_TENSION-MEMBERS_BROCHURE_EN.PDF)
- [16] PN-EN 12385-1 + A1: Steel wire ropes. Safety. Part 1: General requirements. Warszawa: Polski Komitet Normalizacyjny, 2009.
- [17] PN-EN 13411-4: Terminations for steel wire ropes. Safety. Part 4: Metal and resin socketing. Warszawa: Polski Komitet Normalizacyjny, 2013.
- [18] Millfield Enterprises (Manufacturing) Limited, WIRELOCK. Technical data manual. 2017. [Online]. <https://www.wirelock.com/wp-content/uploads/2016/02/Wirelock-Technical-Data-Manual-2-11-17.pdf>
- [19] PN ISO 3108: Steel wire ropes for general purposes. Determination of actual breaking load. Warszawa: Polski Komitet Normalizacyjny, 1996.
- [20] Eurocode 3. PN-EN 1993-1-11: Design of steel structures. Part 1–11: Design of structures with tension components. Warszawa: Polski Komitet Normalizacyjny, 2008.
- [21] Chr. Petersen, *Stahlbau*. Vieweg, Braunschweig/Wiesbaden, 1993.
- [22] U. Peil, “Bauen mit Seilen”, in *Stahlbau-Kalender*. 2000, pp. 690–755.
- [23] A. Der Kiureghian, J.L. Sackman, “Tangent geometric stiffness of inclined cables under self-weight”. *Journal of Structural Engineering ASCE*, 2005, vol. 131, no. 6, pp. 941–945, DOI: [10.1061/\(ASCE\)0733-9445\(2005\)131:6\(941\)](https://doi.org/10.1061/(ASCE)0733-9445(2005)131:6(941)).
- [24] SOFiSTiK 2016 FEA. Oberschleissheim, Germany 2016.
- [25] Eurocode 1. PN-EN 1991-1-4: Actions on structures. Part 1–4: General actions – Wind actions. Warszawa: Polski Komitet Normalizacyjny, 2008.

## Analiza parametryczna odciągów masztu w zakresie sprężystym i pozasprężystym

**Słowa kluczowe:** badania doświadczalne liny, globalna analiza statyczna, nieliniowość fizyczna, nieliniowość geometryczna, odciąg masztu

### Streszczenie:

Praca dotyczy obliczeń odciągów masztu z uwzględnieniem zarówno nieliniowości geometrycznej, jak i fizycznej. Przeprowadzono badania doświadczalne pewnej liny spiralnej. Celem badań było określenie zależności  $\sigma - \varepsilon$  liny (naprężenia – odkształcenia) oraz ustalenie modułu sprężystości liny po jej wstępnym przeciągnięciu. Wyniki badań wykorzystano do utworzenia odpowiednich modeli obliczeniowych cięgien w zakresie sprężystym i pozasprężystym w środowisku programu SOFiSTiK, opartym o FEM. Modele obliczeniowe cięgna posłużyły do przeprowadzenia parametrycznej analizy porównawczej cięgna płaskiego, cięgna ukośnego oraz kratowego masztu z odciągami. Rezultaty obliczeń pojedynczych cięgien uzyskane w programie SOFiSTiK skonfrontowano z wynikami uzyskanymi metodą analityczną, na podstawie równania cięgna (techniczna teoria cięgna). Uzyskane wyniki okazały się zadowalające – różnice w obliczonych wartościach sił naciągu cięgna  $S$  w obu przykładach dla  $E = \text{const}$  nie przekraczały 1%. Dla  $E \neq \text{const}$  różnice były nieco większe (około 2%), co można uzasadnić różnymi iteracyjnymi metodami przybliżonego rozwiązania. Niezależnie od kąta nachylenia cięciwy cięgna do poziomu, wyniki obliczeń cięgien w zakresie liniowo sprężystym i pozasprężystym różnią się istotnie. W pierwszym przypadku cięgna charakteryzują się mniejszymi odkształceniami i większymi siłami naciągu, a w drugim – większymi odkształceniami i mniejszymi siłami naciągu. Ponadto w linach pojawiają się trwałe odkształcenia (im większe obciążenie, tym większe wartości tych odkształceń), które nie znikają po odciążeniu. W przypadku masztów z odciągami zjawisko to może być na tyle niebezpieczne, że może spowodować znaczne zmniejszenie sztywności konstrukcji i utratę jej pionowości, a tym samym niekorzystnie wpłynąć na właściwości użytkowe masztu. Jak pokazuje praktyka projektowa, wstępne rozciąganie nowych lin o dużych długościach i średnicach jest często trudne do wykonania. Dlatego uzasadnione jest przeprowadzenie analiz konstrukcji masztów z uwzględnieniem nieliniowości fizycznej odciągów w przypadku, gdy odciąg wykonano z lin bez wstępnego przeciągnięcia.

Przedstawione w artykule wyniki obliczeń dotyczą określonego typu lin stalowych, które były badane w warunkach laboratoryjnych i nie należy ich uogólniać. W przypadku lin stalowych o innej konstrukcji efekty nieliniowe mogą być inne – im więcej drutów w linie, tym charakterystyka naprężenia – odkształcenia jest bardziej nieliniowa. Uniwersalny charakter ma natomiast przedstawiona w pracy metoda postępowania w przypadku wykorzystania do konstrukcji lin bez wstępnego przeciągnięcia.

Received: 16.04.2021, Revised: 27.07.2021